ELSEVIER

Polymer 44 (2003) 1309–1314

polymer

www.elsevier.com/locate/polymer

Polymer Communication

Electrospinning of a micro-air vehicle wing skin

K.J. Pawlowski*, H.L. Belvin, D.L. Raney, J. Su, J.S. Harrison, E.J. Siochi

NASA, Langley Research Center, Hampton, VA 23681, USA

Received 23 July 2002; received in revised form 8 November 2002; accepted 14 November 2002

Abstract

Electrospinning was utilized to create lightweight, electrically responsive wing skins for micro-air vehicle (MAV) wing frame designs. Various compositions of an electroactive polymer were investigated to determine the appropriate electrospinning conditions for these materials. Electrospun mats of these materials were characterized via optical microscopy and scanning electron microscopy. Tensile properties of the electrospun fibers were also measured. An optimal polymer composition was electrospun onto MAV wing frames to create a bird wing-like texture. Preliminary testing of electroactivity of these prototype MAV wings is reported here.

Keywords: Electrospinning; Electroactive polymers; Micro-air vehicle

1. Introduction

Electrospinning was used to fabricate a wing for micro-air vehicle (MAV) designs. MAVs are small, lightweight vehicles valued for their versatility and mobility [1,2]. They are useful for collecting and transmitting visual images from hazardous locations. Most MAV designs rely on scaled down versions of conventional fixed wing aircraft, incorporating a flexible wing structure consisting of a graphite fiber composite frame covered with a latex skin [3]. The goal of this work was to investigate the viability of electrospinning a lightweight, tailorable wing skin that will permit mimicry of the agility and versatility in control exhibited by birds in flight.

Electroactive polymers (EAPs) have been investigated for use as actuators and artificial muscle because they respond mechanically to an electric field [4,5]. Processing of EAPs via electrospinning introduces the potential for designing an active wing that can be tailored to achieve flight adjustments such as turns and elevation changes in MAV applications. The fibers that can be manufactured via the electrospinning process are much smaller in diameter and, therefore, much lighter with a larger surface area per length than those produced by conventional fiber spinning techniques, thus responding to the need of MAV designers for aircraft that weigh less than 50 g. Furthermore, the application of an electric field during processing introduces the prospect of fiber orientation to optimize actuation capability of the electrospun material.

The electrospinning process is shown schematically in Fig. 1. A polymer solution is charged via a connection to a high voltage power supply and dispensed from a small opening (usually a needle or pipette tip). Because of its charge, a thin jet of this solution is ejected from the tip of the opening and drawn toward a grounded target. As the jet travels toward the collector, the solvent evaporates, depositing a nonwoven fiber mat on the target. These mats are typically composed of very small fibers with diameters ranging from hundreds of nanometers to a few microns.

Lord Rayleigh first reported the fundamental principle of electrospinning in the late 1800s as part of his investigation into the process of electrospraying. He determined the charge necessary to eject a droplet at the end of a nozzle as a stream [6]. In the 1960s, electrospinning was revisited by Taylor, who elucidated the transformation from a droplet to a stream [7,8]. In both studies, it was concluded that stream formation was dependent on the charge density on the droplet overcoming the surface tension. Following the fundamental work of Rayleigh and Taylor, most electrospinning efforts have focused on exploring the types of materials that can be spun using this process and the conditions required to decrease fiber diameters [8–21]. Attention is now shifting toward analysis of the important factors that contribute to electrospinning [8,17–19,22–25]. These investigations range from development of mathematical models

* Corresponding author. Tel.: +1-757-864-5042; fax: +1-757-864-8312.
E-mail address: k.j.pawlowski@larc.nasa.gov (K.J. Pawlowski).

0032-3861/03/$ - see front matter © 2002 Elsevier Science Ltd. All rights reserved.
PII: S0032-3861(02)00859-5

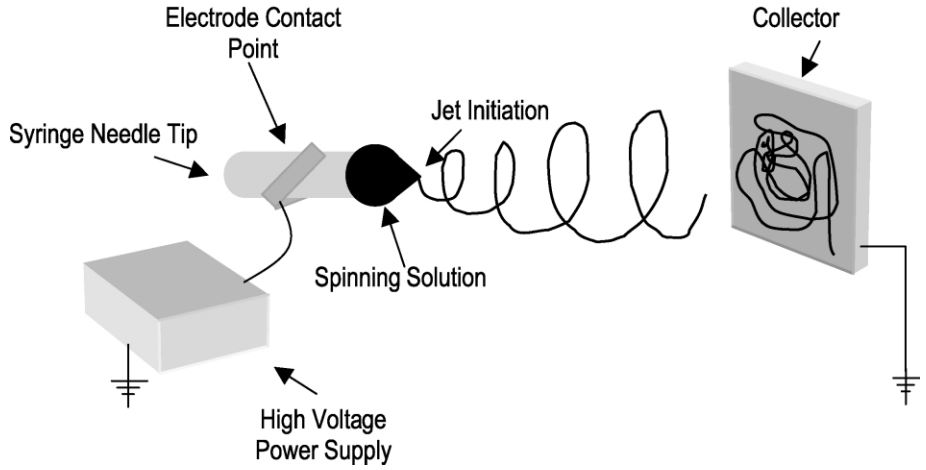

Fig. 1. Schematic of the electrospinning equipment set-up.

describing the travel of the fiber jet to modification of the electrospinning instrumentation to improve some facet of the process or product [26–31].

2. Experimental

The electrospinning set-up was completely self-contained and mobile. A benchtop fume hood (Flow Sciences, Inc.), which utilized the building fume ventilation system, housed the equipment. A high voltage power supply (Spellman High Voltage Electronics Corp.) charged a polymer solution contained in a syringe with a voltage in the range of 0–30 kV via an alligator clip attached to the syringe needle. At some distance from the needle tip, a grounded collector was suspended so that the two were parallel. Fibrous mat buildup depended on a continuous supply of polymer solution to the needle tip via a syringe infusion pump set to provide a desired rate of delivery.

Selection of the most suitable EAP for the required design objectives of the wing coating was a significant part of this project. It was desirable to have a tough, durable, and easily processable polymer capable of reacting quickly with high strain and mechanical output [32,33]. Various types of EAP blends, ranging from piezoelectric polymers to electrostrictive elastomers and copolymers of these materials, were prepared utilizing dimethyl formamide (DMF) as a solvent. These solutions were electrospun to determine the most appropriate composition for this application. The major factor in polymer choice was fiber quality, especially as they spanned the supports of the wing frame.

Optical micrographs were obtained using an Olympus BH-2 coupled to Scion Image, v. 1.62c, software for image capture. Scanning electron micrographs were completed on a JEOL JSM 6400. Mechanical testing was performed using a Satec APEX T1000 test frame in conjunction with Satec Partner, v. 3.0a, analysis software. ASTM D882-01: Standard Test Method for Tensile Properties of Thin Plastic Sheeting was utilized as a guide for mechanical testing.

Following electrospinning and basic analyses, preliminary actuation testing was completed on the electrospun MAV wings. To accomplish this, AC was applied to the wing via attached leads. Waveform and frequency selection was optimized to evoke the largest response from the wing for identification of its resonant frequency.

Three types of copolymers were investigated. Compositions are shown in Table 1 with the modulus measured for the polymer film. Modulus for poly(vinylidene fluoride) (PVDF) was measured for comparison and validation of testing methods; results compared favorably with published data [34].

3. Results and discussion

A piezoelectric copolymer of PVDF and trifluoroethylene (TrFE) was investigated. This copolymer was chosen

Table 1
Tensile modulus of polymer films

Material	Backbone	Elastic modulus (MPa)
Copolymer	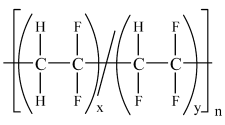	338 ± 40
GE	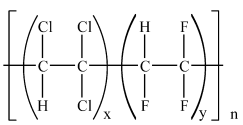	169 ± 9
TrF1	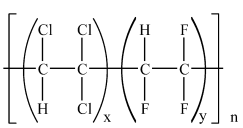	86 ± 1
PVDF	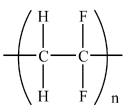	3000 ± 590

because it offers a higher crystallinity than PVDF alone and it is not necessary to stretch the material to induce a polar crystalline phase [35]. Fig. 2 shows a typical optical microscope image of electrospun piezoelectric copolymer showing more globular masses than fibrous material. At lower magnification, a wet coating was observed, indicating prevalence of polymer spraying versus fiber spinning. However, at higher magnification, some fiber deposition was evident amongst the polymer droplets. Additionally, agglomeration was apparent at some junction points of the fibers; this feature demonstrates that the fibers were not completely dry upon deposition.

An optical micrograph of spun Graft Elastomer (GE) is illustrated in Fig. 3. This material consists of a random poly(trichloroethylene–trifluoroethylene)-based flexible backbone with the addition of randomly-grafted crystalline polarizable PVDF end groups, which provide crosslinking sites to help retain elastomeric properties [32]. The materials are of interest because they offer high strain capability and are easy to process. Predominantly fibrous mats with fiber diameters ranging from 2 to 3 μm were obtained with favorable spinning conditions. However, minor changes in any of the spinning parameters yielded widely different mat quality.

Trifluoro Graft Elastomer (TrF1) (patent pending) copolymer is a variation of GE in which the grafted segments are the piezoelectric copolymer discussed above. This modification results in lower induced strain capability compared to GE. Electrospinning of solutions of this material under a variety of conditions demonstrates the effect that spinning parameters have on the final arrangement and quality of the fibers.

The effect of varying voltage is shown in Fig. 4. At low voltage, a smaller proportion of fibers versus nonfibrous masses was evident. Furthermore, the fibers were not as dry as desired. As voltage was increased, however, the proportion of fibers increased, and fibers were better defined and drier.

Distance between the jet initiation point and target had significant effects on fiber formation. The micrographs shown in Fig. 4 are of samples that were electrospun at a

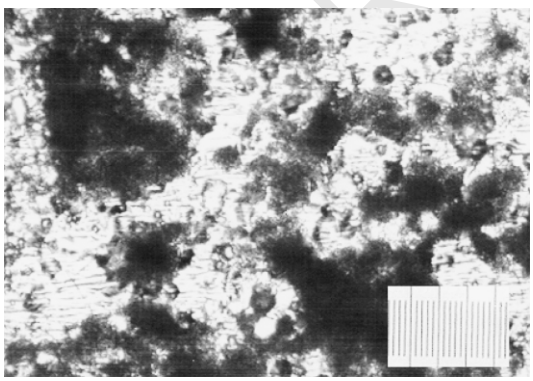

Fig. 2. Optical micrograph of electrospun mat of piezoelectric copolymer. Each division is 10 μm.

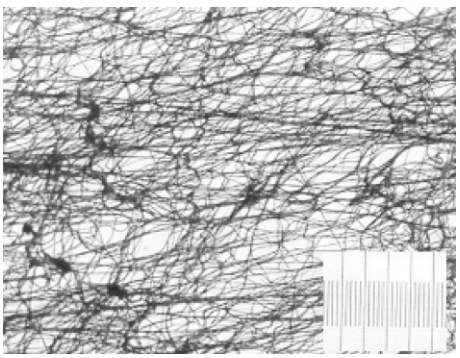

Fig. 3. Electrospun GE at 13 wt% concentration. Each division is 10 μm.

distance of only 7.6 centimeters (cm) between the jet initiation point and target, which was too close for optimal fiber formation of this polymer composition. Fig. 5 shows micrographs of TrF1 electrospun at two different distances under otherwise optimal conditions. At a distance of 7.6 cm, nonfibrous masses were predominant and fibers that did form were wet. If distance were increased to 25.4 cm, fibers were predominant and very dry. In addition, fiber morphology and diameter were uniform.

Solution properties including concentration and molecular weight, which both contribute to final viscosity, also led to major differences in mat properties. In these investigations, molecular weight was held constant, and concentration was varied. Fig. 6 shows the effect of concentration

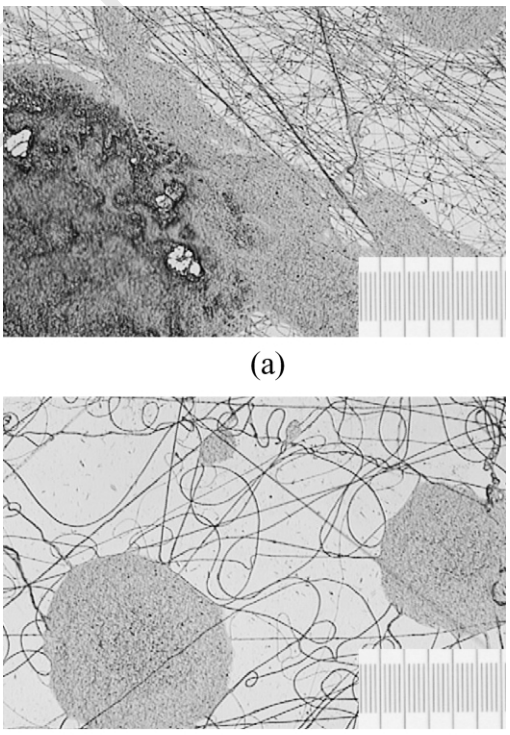

Fig. 4. As voltage was increased from (a) 12 V to (b) 25 V, the proportion of fibers increased, and fibers were more defined and drier. Each division is 10 μm.

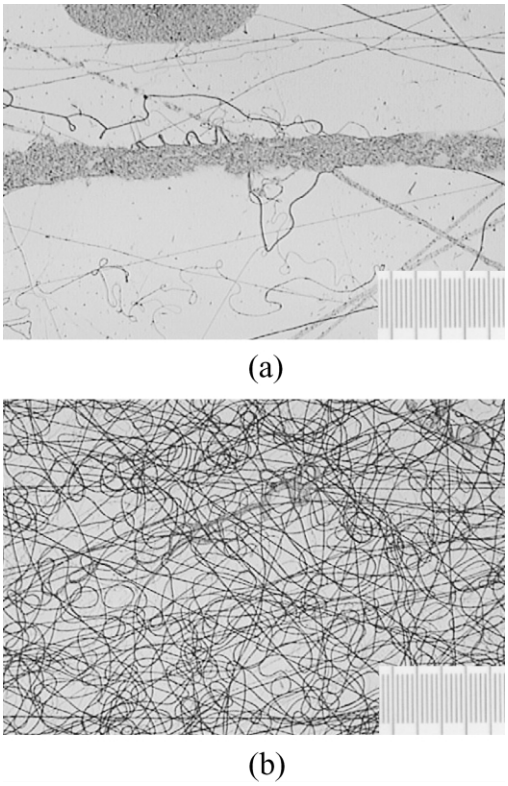

Fig. 5. As distance was increased from (a) 7.6 cm to (b) 25.4 cm, fibers were predominant, and morphology and diameter were regular. Each division is 10 μm.

on electrospun mat characteristics. At 10 weight percent (wt%), the entire collected sample was a nonfibrous mass of wet droplets. At 16 wt%, some evidence of fiber formation was obvious; these fibers were very tiny with diameters of about 500 nm. However, the sample still exhibited holes or open regions where it appeared that sprayed wet solution droplets deposited on the mat and redissolved some of the preformed fibers. At 20 wt%, fibers were much more defined, drier, and had larger diameters. This transition from sprayed wet droplets to spun dry fibers is typical as optimal concentration for electrospinning is ascertained.

Fig. 7 shows scanning electron micrographs of TrF1 electrospun at optimal conditions. A series of samples was spun, resulting in various fiber morphologies. The inset in Fig. 7(a) shows that flat ribbons can be fabricated in contrast to the predominantly cylindrical fibers observed in Fig. 7(b). Fig. 7(a) and (b) also reveal the formation of agglomerations of varying degrees. Occasionally, droplets were visible. Fiber diameters ranged from 200–300 nm to 3–4 μm. Conditions required for the formation of cylindrical versus flat ribbons are currently under investigation.

TrF1 was electrospun from solution to examine its capacity to cover an open target such as the MAV wing frame. The wing frame was mounted to the front of the flat grounded target, and fibers were allowed to deposit randomly onto the wing frame. Once a significant amount of fiber had accumulated, the frame was removed from the

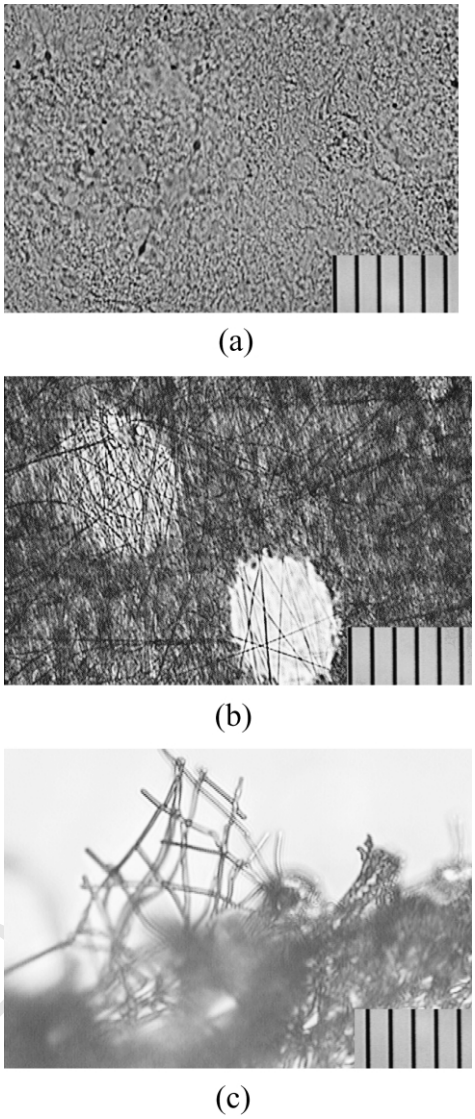

Fig. 6. Changes in fiber formation characteristics and properties were evident with an increase in solution concentration: (a) 10 wt%, (b) 16 wt%, and (c) 20 wt%. Each division is 10 μm.

grounded collector, flipped over, and remounted to spin fibers onto the other side of the frame. Fig. 8 shows the spun wings.

TrF1 fibers covered the wing frame forming a mat and remained securely attached and intact when the frame was removed from the collector. The resulting fibrous coatings exhibited a degree of strength and elasticity consistent with the small diameter of the individual fibers and the complex network that the fibers created. Mechanical testing ($n = 10$) of electrospun mats of these materials confirmed this

Table 2
Mechanical properties of electrospun TrF1 ($n = 10$)

Mechanical property	TrF1
Elastic modulus (MPa)	14.8 ± 2.4
Elongation at break (%)	90.5 ± 27.3

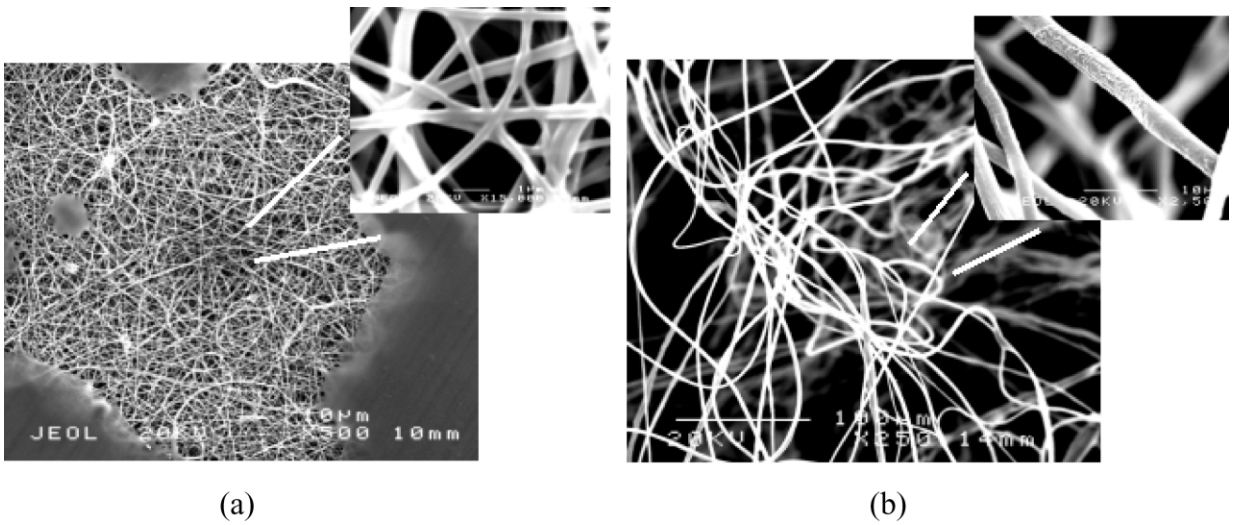

Fig. 7. Scanning electron microscopy (SEM) micrographs of electrospun fibers of TrF1. (a) Mat and (b) detail of fibers. Note cylindrical and flat fiber morphology and agglomerations.

observation. See Table 2. Elastic modulus was calculated as the slope of the linear region of the stress versus strain curve. Elongation at break was determined from peak strain. The electrospun fibrous mats had an expected property knockdown compared to the film, which exhibited a stiffness of 86 ± 1 MPa and an elongation of 985 ± 29%. This was anticipated due to the fibrous nature of the mats. The electrospun fibers created an unoriented mesh, with bonded contact points between fibers. Upon elongation, contact points in the mat were broken, and, finally, fibers were broken. As the mats were pulled in tension, contributions from mesh properties as well as fiber properties were observed. In preliminary attempts at fiber actuation, the fiber-coated wing frames exhibited a perceptible vibration upon excitation with a 2 kV (peak-to-peak) sine wave at 6.7 Hz.

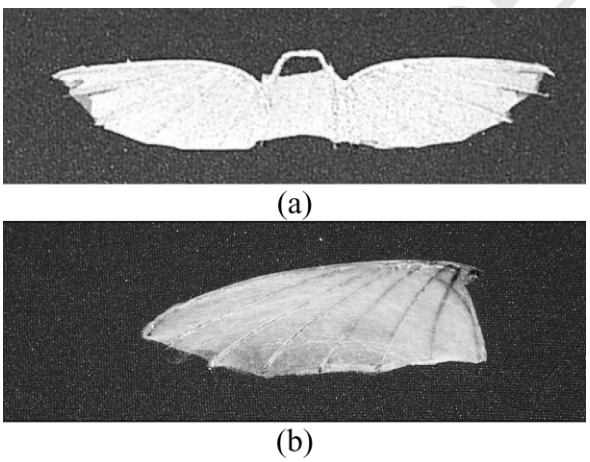

Fig. 8. TrF1 fibers electrospun onto MAV wing frames. (a) Double wing configuration, approximate dimensions are 15.2 cm × 5.1 cm;. (b) Single wing configuration, approximate dimensions are 10.2 cm × 6.4 cm.

4. Conclusions

These positive results confirm the feasibility of utilizing electrospinning to process novel EAPs for the fabrication of lightweight, responsive MAV wings. A useful polymer-solvent system was identified, electrospinning conditions for this system were determined, and preliminary characterization of the resulting mats was completed. Future work will concentrate on optimization of the spinning solution composition with attention to properties such as conductivity and surface tension, equipment modifications to control fiber deposition and orientation, and further investigations into the activation and actuation properties of the fibers, fiber mats, and electrospun wing frames.

Acknowledgements

The authors would like to thank James Baughman for his assistance in obtaining the SEM micrographs presented, Central Glass, Inc., for providing some of the materials used in this work, and Dr Gary L. Bowlin for his guidance in setting up our electrospinning apparatus.

References

[1] Morris SJ, Holden M. Proceedings of Conference: Fixed flapping and rotary wing vehicles; 2000. p. 153–75.
[2] Latek B, Reed H, Saric W. Proceedings of Conference: Fixed flapping and rotary wing vehicles; 2000. p. 478–85.
[3] Ifju PG, Jenkins DA, Ettinger S, Lian Y, Shyy W, Waszak MR. AIAA, 2002-0705; 2002.
[4] Pelrine RE, Kornbluh RD, Joseph JP. Sens Actuators A 1998;64: 77–85.
[5] Otero TF, Sansinena JM. Adv Mater 1998;10:491–4.

[6] Rayleigh L. London, Edinburgh, and Dublin. Phil Mag 1882;14: 184–6.
[7] Taylor G. Proc R Soc London A 1969;313:453–75.
[8] Doshi J, Reneker DH. J Electrostatics 1995;35:151–60.
[9] Reneker DH, Chun I. Nanotechnology 1996;7:216–23.
[10] Srinivasan G, Reneker DH. Polym Int 1995;36:195–201.
[11] Liu W, Wu Z, Reneker DH. Polym Prepr 2000;41:1193–4.
[12] Chun I, Reneker DH, Fong H, Fang X, Deitzel J, Beck Tan N, Kearns K. J Adv Mater 1999;31:36–41.
[13] Fong H, Chun I, Reneker DH. 24th Biennial Conference on Carbon; 1999. p. 380–1.
[14] Fong H, Chun I, Reneker DH. Polymer 1999;40:4585–92.
[15] Schreuder-Gibson H, Senecal K, Sennett M, Huang Z, Wen J, Li W, Wang D, Yang S, Tu Y, Ren Z, Sung C. Proceedings of the 197th meeting of the electrochemical society, Fullerenes 2000: Chemistry and physics of fullerenes and carbon nanomaterials; 2000. p. 210–21.
[16] Zarkoob S, Reneker DH, Ertley D, Eby RK, Hudson SD. US Patent 6, 110,590; 2000.
[17] Deitzel JM, Beck Tan NC, Kleinmeyer JD, Rehrmann J, Tevault D, Reneker D, Sendijarevic I, McHugh A. ARL-TR-1989; 1999.
[18] Deitzel JM, Kleinmeyer JD, Harris D, Beck Tan NC. Polymer 2001; 42:261–72.
[19] Bognitzki M, Frese T, Wendorff JH, Greiner A. Proceedings of the American Chemical Society, Division of Polymeric Materials: Science and Engineering; 2000. p. 115–6.
[20] Drew C, Wang X, Senecal K, Schreuder-Gibson H, He J, Tripathy S, Samuelson L. 58th Annu Tech Conf-Soc Plast Eng; 2000. p. 1477–81.
[21] MacDiarmid AG, Jones Jr WE, Norris ID, Gao J, Johnson Jr AT, Pinto NJ, Hone J, Han B, Ko FK, Okuzaki H, Llaguno M. Synth Met 2001; 119:27–30.
[22] Jaeger R, Bergshoef MM, Martin i Batlle C, Schonherr H, Vancso GJ. Macromol Symp 1998;141–50.
[23] Kim J, Lee DS. Polym J 2000;32:616–8.
[24] Gibson PW, Schreuder-Gibson HL, Rivin D. AIChE J 1999;45: 190–5.
[25] Gibson P, Schreuder-Gibson H, Pentheny C. J Coat Fabrics 1998;28: 63–72.
[26] Reneker DH, Yarin AL, Fong H, Koombhongse S. J Appl Phys 2000; 87:4531–47.
[27] Warner SB, Ugbolue SC, Patra PK, Buer A, Kalayci VE, Kim YK. New Frontiers Fiber Sci 2001;37–8.
[28] Hohman MM, Shin M, Rutledge G, Brenner MP. Phys Fluids 2001; 13:2201–20.
[29] Hohman MM, Shin M, Rutledge G, Brenner MP. Phys Fluids 2001; 13:2221–36.
[30] Ali A, Geshury A, Ko F. New Frontiers Fiber Sci 2001;30.
[31] El-Aufy A, Ko F. New Frontiers Fiber Sci 2001.
[32] Su J, Harrison JS, St Clair TL, Bar-Cohen Y, Leary S. Electroactive polymers. Materials Research Society Symposium; 1999. p. 131–6.
[33] Su J, Ounaies Z, Harrison JS, Bar-Cohen Y, Leary S. Electroactive polymer actuators and devices. Smart structures and materials; 2000. p. 65–72.
[34] Kepler RG. In: Nalwa HS, editor. Ferroelectric polymers: chemistry, physics and applications. New York: Marcel Dekker; 1995. p. 183–232.
[35] Furukawa T. IEEE Trans Electric Insul 1989;24:375–94.